IDENTIFICATION OF "CHOCOLATE PEARLS" TREATED BY BALLERINA PEARL CO.

Wuyi Wang, Kenneth Scarratt, Akira Hyatt, Andy Hsi-Tien Shen, and Matthew Hall

Treated cultured pearls with a "chocolate" coloration have entered the market from several sources. Gemological, spectroscopic, and chemical analyses were performed on both untreated and treated cultured pearls to provide a better understanding of the "chocolate" treatment process that is used by one company (Ballerina Pearl Co.) and to determine how these products can be identified. It is likely that the organic components in black cultured pearls were bleached to create the brown coloration; no foreign coloring agent was detected. Cultured pearls treated by this method can be identified based on their unusual coloration, characteristic fluorescence, UV-Vis-NIR reflectance and Raman spectra, and trace-element composition.

To achieve an attractive and consistent color appearance, cultured pearls are frequently treated by bleaching, dyeing (such as with silver nitrate), or exposure to radiation. A "new" color for cultured pearls was introduced to the market in 2000 (figure 1; see, e.g., "U.S. gem labs…," 2004; Zachovay, 2005; "GIA identifies…," 2006; Strack, 2006; "Study shows…," 2006). The induced brown color reportedly results from the bleaching of "black" Tahitian cultured pearls. These are now known in the trade as "chocolate pearls" and have become quite popular (Sanchez, 2004). They are available from several sources, including Ballerina Pearl Co. in New York and Shanghai Gems SA in Geneva ("Better techniques," 2006). The companies treating these cultured pearls assert that no color is added during treatment (Sanchez, 2004). However, it is unlikely that all the "chocolate pearls" marketed today have been treated using the same technique.

To better understand the treatment process being used by one company (Ballerina Pearl Co.) and how these new products can be identified, we analyzed the gemological, chemical, and spectroscopic properties of several of these "chocolate pearls" as well as silver-dyed Tahitian cultured pearls and untreated gray and brown Tahitian cultured pearls. In addition, we asked Ballerina Pearl Co. to treat four Tahitian cultured pearls specifically for this study.

MATERIALS AND METHODS

A total of 196 cultured pearls weighing 3.75–21.40 ct (9.5–19.7 mm in diameter) were selected for this study (see, e.g., figure 2; a representative list is given in table 1). These included 29 natural-color Tahitian cultured pearls (NCTCP) from GIA's collection that were obtained directly from pearl farmers. Of these, 19 were dominated by gray coloration and the other 10 by brown coloration. These samples have been in GIA's collection for at least five years, and the laboratory confirmed that they were natural color. The "chocolate" cultured pearls (CCP; 160 samples) and silver [Ag]-dyed Tahitian cultured pearls (DTCP; three samples) were supplied by Ballerina Pearl Co. and its distributor Emiko Pearl International. We cut through the nacre of two CCPs (Bal-12 and Bal-13) to examine color variation with depth.

See end of article for About the Authors and Acknowledgments.
GEMS & GEMOLOGY, Vol. 42, No. 4, pp. 222–235.

Figure 1. Samples of intense brown "chocolate pearls" are shown in this necklace (12.0–13.7 mm) and ring (12.9 mm) that Ballerina Pearl Co. has produced from Tahitian black cultured pearls with their proprietary treatment process. Natural-color Tahitian cultured pearls with dominant brown coloration are rare. Courtesy of Emiko Pearls International; photo by Robert Weldon.

Details of the treatment remain proprietary, but Ballerina Pearl Co. did disclose that two steps are involved (A. Auerbach, pers. comm., 2006). At our request, Ballerina Pearl Co. subjected four representative undrilled NCTCPs (samples Bal-02, Bal-16, Bal-18, Bal-19) to their two-step treatment process to induce the "chocolate" color. We examined three of them after each of the two steps; sample Bal-02 was only examined after the final step.

The color of all samples was described in accordance with the GIA pearl classification system (Gemological Institute of America, 2000). Visual features were observed using a standard gemological microscope. Reactions to UV radiation were checked in a darkened room with conventional 4-watt long-wave (366 nm) and short-wave (254 nm) lamps.

Infrared reflectance spectra were recorded for 46 samples (all 29 NCTCPs, 10 CCPs of varying colors, three DTCPs, and the four NCTCPs studied before and after treatment). The spectra were collected in the mid-infrared region (6000–400 cm^{-1}; 1.0 cm^{-1} resolution) at room temperature with a Thermo-Nicolet Nexus 670 Fourier-transform infrared (FTIR) spectrometer equipped with a KBr beam splitter and MCT-B detector. Instead of using the destructive KBr pellet method, we employed a diffuse reflectance technique that focuses the incident infrared beam on the sample's surface. Diffused light traveling through the outermost layer provides information about the absorption characteristics of that sample. A total of 512 scans (per spectrum) were collected to improve the signal-to-noise ratio.

Reflectance spectra in the UV-Vis-NIR range of 190–850 nm were collected on 98 samples (all 29 NCTCPs, 62 CCPs of varying colors, three DTCPs, and the four samples examined before and after treatment) using a PerkinElmer Lambda 950 spectrometer at room temperature (step interval = 0.25 nm; slit = 2.0 nm). A black metal disk with a center hole of ~6.0 mm in diameter was used to select a specific area of each cultured pearl for analysis while securing the sample against the light integration sphere.

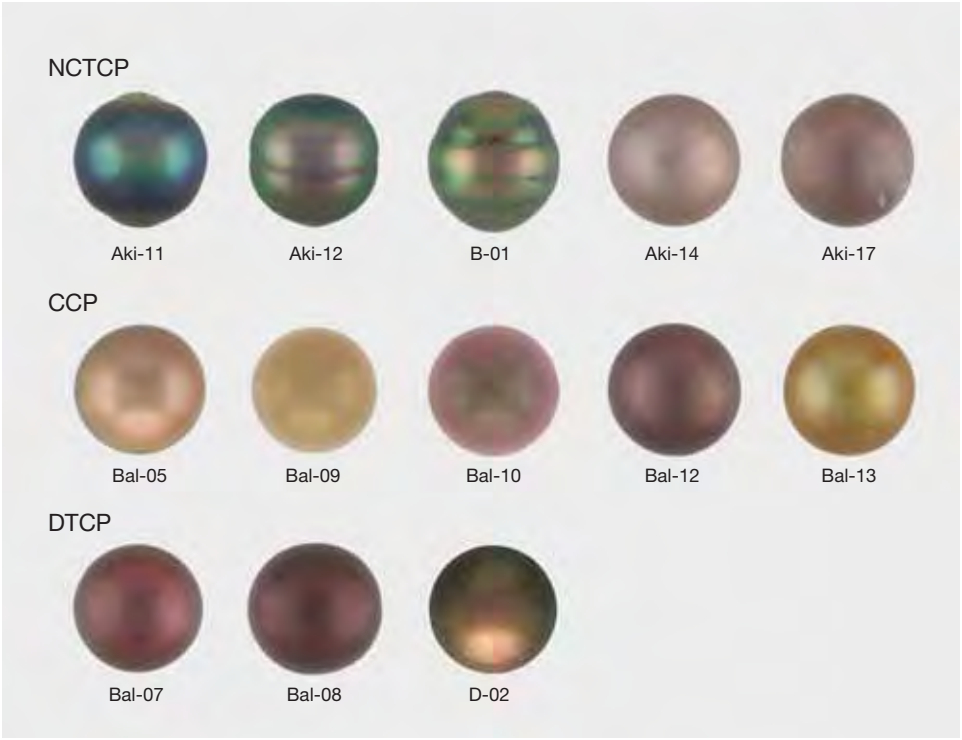

Figure 2. Shown here are some of the cultured pearls (9.05–13.47 mm in diameter) examined as part of this study (top row, natural color; middle row, treated "chocolate" color; bottom row, silver nitrate dyed). Photos by Jessica Arditi and Jian Xin (Jae) Liao.

Raman and photoluminescence spectra of 37 samples (19 NCTCPs of both gray and brown colors, 11 CCPs of varying colors, three DTCPs, and the four samples examined before and after treatment) were recorded at room temperature using a Renishaw inVia Raman microspectrometer that was equipped with an Ar-ion laser operating at two excitation wavelengths (488.0 and 514.5 nm) and a He-Nd laser with 632.8 nm excitation. We calibrated the instrument using the Raman shift of a single-crystal silicon reference. Initial laser power was adjusted for maximum signal intensity while avoiding oversaturation. Up to 10 scans per spectrum were collected to improve the signal-to-noise ratio.

Chemical composition was determined qualitatively with a Thermo-Noran Spectrace QuanX energy-dispersive X-ray fluorescence (EDXRF) spectrometer, and quantitatively using a Thermo X Series inductively coupled plasma–mass spectrometer (ICP-MS) combined with a New Wave UP213 laser ablation system for sampling. We analyzed 47 samples (all 29 NCTCPs, 11 CCPs of varying colors, three DTCPs, and the four samples examined before and after treatment) using EDXRF, and 70 cultured pearls (27 NCTCPs, 38 CCPs, two DTCPs, and three samples examined before and after treatment) using LA-ICP-MS. For EDXRF analysis, all X-ray filter options (none, cellulose, Al, thin Pd, medium Pd, thick Pd, thin Cu, and thick Cu) were applied individually with accelerating voltages of 8, 10, 12, 20, 20, 28, 50, and 50 kV, respectively. A collimator of 3.5 mm diameter was used. Beam current was automatically controlled to maintain a 50% dead time in data collection. Live time for data accumulation was 100 seconds. All spectra were collected at ~0.01 Pascal. For the LA-ICP-MS analysis, a laser beam with a wavelength of 213 nm was rastered across the pearl surface along a 1–2 mm line (figure 3). The

Figure 3. This scanning electron microscope image of a NCTCP (Aki-01) shows the platelet structure of the nacre and the effects of the laser penetration into the nacre during LA-ICP-MS analysis. A minute depression with a length of ~1 mm, width of 40 μm, and depth of ~20 μm was created during the analysis.

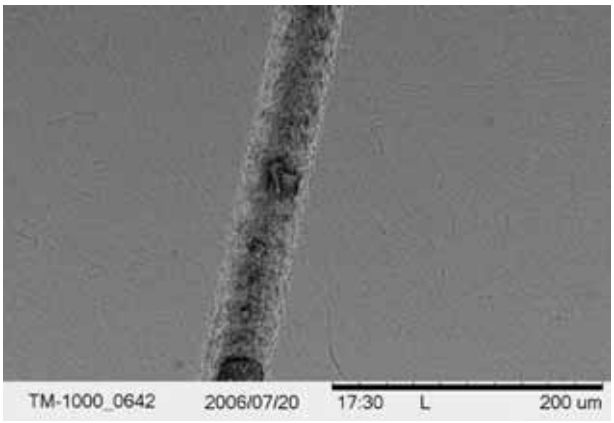

TABLE 1. Representative samples of natural-color Tahitian, "chocolate," and silver-dyed Tahitian cultured pearls examined for this study.

Sample no.	Color	Luster	Surface (extent of spotting)	Size (mm)	Fluorescence to UV radiation	
					Long-wave	Short-wave
Natural-Color Tahitian Cultured Pearls (NCTCPs)						
Aki-01	Greenish gray	High	Heavy	~10.11–10.39	Weak greenish yellow	Weak greenish yellow
Aki-02	Black	High	Moderate	~10.66–14.14	Very weak orange	Very weak greenish yellow
Aki-03	Gray and greenish gray	Medium	Light	~12.29–19.74	Weak orange	Very weak greenish yellow
Aki-04	Dark greenish gray (with rosé)	High	Heavy	~11.62–13.01	Very weak orange	Very weak greenish yellow
Aki-05	Greenish gray	Medium	Moderate	~13.54–17.46	Very weak orange	Very weak greenish yellow
Aki-06	Dark greenish gray (with orient)	High	Light	~11.10–16.37	Very weak yellow	Very weak greenish yellow
Aki-07	Dark greenish gray (with rosé)	High	Moderate	~10.41–12.48	Inert	Inert
Aki-08	Dark greenish gray (with rosé and orient)	High	Heavy	~11.22–13.49	Very weak yellow	Very weak greenish yellow
Aki-09	Dark greenish gray (with rosé)	High	Moderate	~10.90–11.80	Very weak orange	Very weak greenish yellow
Aki-10	Dark greenish gray	Medium	Heavy	~12.56–14.96	Very weak orange	Very weak greenish yellow
Aki-11	Dark violetish gray	High	Heavy	~9.50–9.56	Inert	Inert
Aki-12	Greenish gray (with rosé)	High	Moderate	~9.05–9.52	Very weak yellow	Very weak greenish yellow
Aki-13	Orangy brown and dark gray	Medium	Moderate	~13.9	Weak greenish yellow	Very weak greenish yellow
Aki-14	Orangy brown	Medium	Heavy	~11.7	Weak yellow	Very weak greenish yellow
Aki-15	Pinkish brown	Medium	Heavy	~11.8	Weak yellow	Very weak greenish yellow
Aki-16	Orangy brown	Medium	Heavy	~12.8	weak orange	Very weak greenish yellow
Aki-17	Pinkish brown	Medium	Heavy	~10.4	Very weak yellow	Very weak greenish yellow
Aki-18	Pinkish brown	Low	Heavy	~12.2	Very weak orange	Inert
Aki-19	Dark brown	High	Moderate	~9.9	Very weak orange	Inert
Aki-20	Dark greenish gray (with rosé)	High	Moderate	~10.0	Very weak yellow	Inert
Aki-21	Orangy brown	Low	Heavy	~11.4	Weak orange	Very weak yellow
Aki-22	Dark brown	Low	Heavy	~10.6	Very weak orange	Inert
Aki-23	Orangy brown	Medium	Heavy	~10.9	Weak orange	Very weak greenish yellow
"Chocolate" Cultured Pearls (CCPs)						
Bal-03	Yellowish brown	High	Light	~11.99–12.05	na[a]	na
Bal-12	Dark brown	Medium	Moderate	~10.0	Very weak reddish orange	Inert
Bal-13	Yellow-brown	Medium	Moderate	~10.8	Moderate reddish orange	Very weak orange
Bal-14	Pink-brown	Medium	Light	~14.0	Moderate reddish orange	Weak orange
Bal-56	Orange-brown	High	na	~12.3	Moderate reddish orange	Weak greenish yellow
Bal-57	Orange-brown	High	na	~12.1	Moderate reddish orange	Weak greenish yellow
Bal-58	Orange-brown	High	na	~11.8	Moderate reddish orange	Weak greenish yellow
Bal-59	Orange-brown	High	na	~12.1	Moderate reddish orange	Weak greenish yellow
Bal-60	Orange-brown	High	na	~12.6	Moderate reddish orange	Weak greenish yellow
Bal-61	Orange-brown (with rosé)	High	na	~12.3	Moderate reddish orange	Weak greenish yellow
Bal-62	Orange-brown (with rosé)	High	na	~11.7	Moderate reddish orange	Weak greenish yellow
Bal-63	Orange-brown	High	na	~12.0	Moderate reddish orange	Weak greenish yellow
Bal-64	Orange-brown	High	na	~12.3	Moderate reddish orange	Weak greenish yellow
Bal-65	Orangy brown	High	na	~13.7	Moderate reddish orange	Moderate greenish yellow
Bal-66	Orange-brown (with rosé)	High	na	~12.2	Moderate greenish yellow	Moderate greenish yellow
Bal-67	Orange-brown (with rosé)	High	na	~12.0	Moderate reddish orange	Weak greenish yellow
Bal-68	Orange-brown	High	na	~12.9	Moderate reddish orange	Weak greenish yellow
Bal-69	Orange-brown	High	na	~12.1	Weak reddish orange	Inert
Bal-70	Dark brown	High	na	~12.2	Weak reddish orange	Inert
Bal-71	Orangy brown	High	na	~12.9	Moderate reddish orange	Weak greenish yellow
Dyed Tahitian Cultured Pearls (DTCPs)						
Bal-07	Dark brownish pink	Medium	Moderate	~10.0–10.5	Inert	Inert
Bal-08	Dark pink-brown	Medium	Moderate	~10.0–10.5	Inert	Inert

[a]*na = not analyzed.*

Figure 4. The induced dark brown color was distributed evenly in the nacre of CCP sample Bal-12 (left, 10.0 mm), which was cut to a depth of ~1 mm. In CCP sample Bal-13 (right, 10.8 mm), yellow-brown color was distributed evenly through most of the outer layer of the nacre (~1.5 mm thick). The same hue, though lighter, was observed in the interface region between the nacre and the nucleus. Photo by Jian Xin (Jae) Liao.

laser rastered across the line only once and the ablation depth was about 20 μm at this condition, which ensured that the composition of only the outermost layer of the nacre was measured.

RESULTS

Gemological Observations. Most of the "black" NCTCPs showed greenish gray to dark greenish gray coloration, which was sometimes inhomogeneous (again, see figure 2). Overtones of violet, blue, yellow, green, and "rosé" were common. Ten of the NCTCPs showed distinct orangy or pinkish brown colors. Good-quality specimens (~70% of samples in this study) typically showed medium-to-high luster.

The CCPs were dominated by a brown coloration, although some also exhibited yellowish, greenish, pinkish, or orangy hues (again, see figure 2). The tone of the brown color varied significantly among samples, from light to very dark. Orient was usually not observed. Similar to the NCTCPs, the CCPs showed medium to high luster. The three DTCP samples exhibited dark brown coloration with clear pink overtones and medium luster.

When the nacre in one dark brown "chocolate pearl" (Bal-12) was cut to a depth of ~1 mm (figure 4, left), we observed that the dark brown color was distributed evenly with depth. However, in the yellow-brown CCP (Bal-13) that was cut ~1.5 mm through the nacre layer into the nucleus (figure 4, right), the hue was distributed evenly throughout most of the outer nacre, but showed lighter tone at the nucleus interface.

Most of the gray NCTCPs fluoresced very weak orange, yellow, or greenish yellow to long-wave UV radiation, and very weak greenish yellow to short-wave UV. The brown NCTCPs displayed very similar reactions. However, the blemishes seen on the surface of most of the brown cultured pearls exhibited strong greenish yellow fluorescence; this was rarely observed in the gray NCTCPs. Of the 160 CCPs tested, the vast majority (157) displayed weak (~60%) to moderate (~40%) chalky reddish orange fluorescence to long-wave UV. This fluorescence

TABLE 2. Gemological features of four samples before and after "chocolate" treatment by Ballerina Pearl Co.

Feature	Bal-02		Bal-16			Bal-18			Bal-19		
	Untreated	Treated	Untreated	Preparatory treated	Treated	Untreated	Preparatory treated	Treated	Untreated	Preparatory treated	Treated
Color	Greenish gray	Greenish brown	Dark brown	Dark brown	Dark brown	Dark greenish gray (with rosé)	Green brown (with rosé)	Orangy brown (with rosé)	Dark greenish gray (with rosé)	Orange-brown	Orangy brown (with rosé)
Luster	Medium	Medium	Medium	Medium	High	Medium	High	High	High	High	High
Surface (extent of spotting)	Light	Light	Heavy	Heavy	Heavy	Moderate	Moderate	Moderate	Moderate	Moderate	Moderate
Size (mm)	~11.41–11.73			~10.22–10.34			~10.65–10.81			~10.95–11.26	
Weight (ct)	10.65	10.64	7.74	7.72	7.71	8.44	8.42	8.40	9.74	9.70	9.69
Fluorescence											
To long-wave UV	Very weak orange	Moderate greenish yellow	Very weak yellow	Very weak reddish orange	Very weak reddish orange	Very weak yellow	Very weak reddish orange	Moderate reddish orange	Very weak yellow	Very weak reddish orange	Moderate reddish orange
To short-wave UV	Very weak greenish yellow	Weak greenish yellow	Inert	Inert	Inert	Very weak greenish yellow	Inert	Very weak greenish yellow	Very weak greenish yellow	Very weak orangy red	Very weak greenish yellow

was not observed in the NCTCPs, and only three CCPs displayed weak-to-moderate greenish yellow or yellow fluorescence to long-wave UV. When exposed to short-wave UV radiation, 156 CCPs showed weak-to-moderate greenish yellow fluorescence (in four, the reaction was inert). No clear correlation between the intensity of fluorescence and the tone of brown color was observed. The three DTCP samples showed no reaction to either long- or short-wave UV.

The variations in major gemological features exhibited by the four cultured pearls treated by Ballerina Pearl Co. for this study are summarized in table 2. Distinct changes in color were induced in the three gray samples (Bal-02, Bal-18, and Bal-19) by the preparatory process, and the brown color was further enhanced in the second step of treatment (figure 5). The hue of dark brown Bal-16 remained basically unchanged, although the tone was reduced, resulting in a more "chocolate" appearance. After treatment, these "chocolate pearls" lost a slight amount of weight (0.1–0.5%) but the blemishes appeared the same. A slight improvement in luster was observed in two of the four specimens (Bal-16 and Bal-18). A notable difference between samples was observed in their long-wave UV fluorescence. In three samples (Bal-16, Bal-18, and Bal-19), it changed from very weak yellow to distinct reddish orange, with an intensity varying from very weak to moderate. In sample Bal-02, it changed from very weak orange to moderate greenish yellow.

Infrared Reflectance Spectroscopy. The NCTCPs displayed consistent absorption features in the mid-infrared region. These features included strong absorption bands at 1514–1506 and 878 cm^{-1} and weak-to-moderate bands at 1780, ~1084, 713, and 700 cm^{-1} (figure 6). The gray and brown NCTCPs showed identical features, which are generally consistent with the mineral aragonite (again, see figure 6), in particular with the occurrence of the peak at 1084 cm^{-1}. However, the peak at 878 cm^{-1} for the NCTCPs is very different from the 860 cm^{-1} peak in aragonite, and occurs at nearly the same position as seen in calcite. As expected, no absorption peaks related to organic components were detected from the NCTCPs. Infrared reflectance yielded nearly identical absorption features for the CCPs and DTCPs as for the NCTCPs (figure 7). The four NCTCPs treated for this study showed no detectable variation in their mid-infrared reflectance spectra after the treatment.

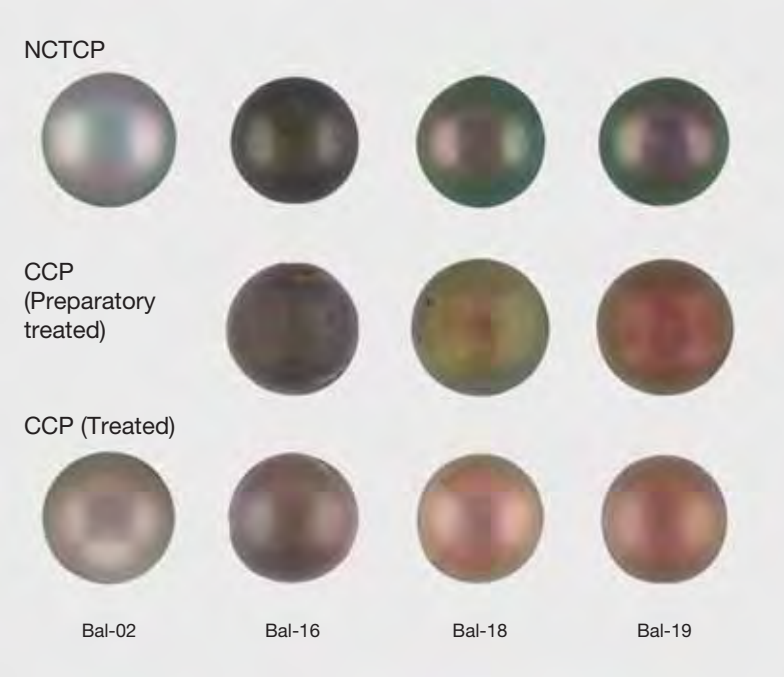

Figure 5. These four Tahitian cultured pearls (top; 10.22–11.73 mm in diameter) were treated by the Ballerina Pearl Co. in a two-stage process to produce "chocolate pearls." An intense brown color was created in the preparatory treatment (middle) and then enhanced in the final step (bottom). Photos by Jessica Arditi and Jian Xin (Jae) Liao.

Figure 6. The mid-infrared reflectance spectra of the NCTCPs are similar to the spectrum of aragonite, in particular with the occurrence of a peak at 1084 cm^{-1}. However, the peak at 878 cm^{-1} for the NCTCPs is much higher in position than the 860 cm^{-1} peak in aragonite, and occurs at nearly the same position as seen in calcite. Gray and brown NCTCPs examined for this study displayed identical absorption features.

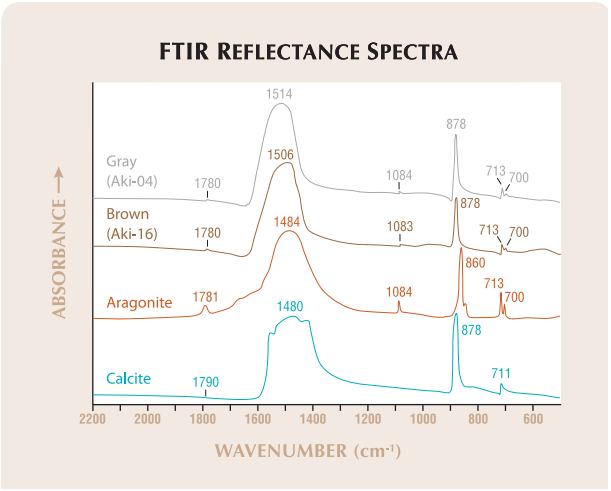

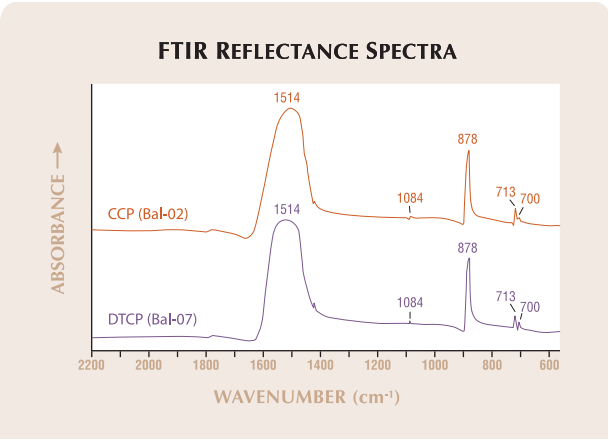

Figure 7. The mid-infrared absorption spectra of the CCPs and DTCPs were nearly identical to those of the NCTCPs in figure 6.

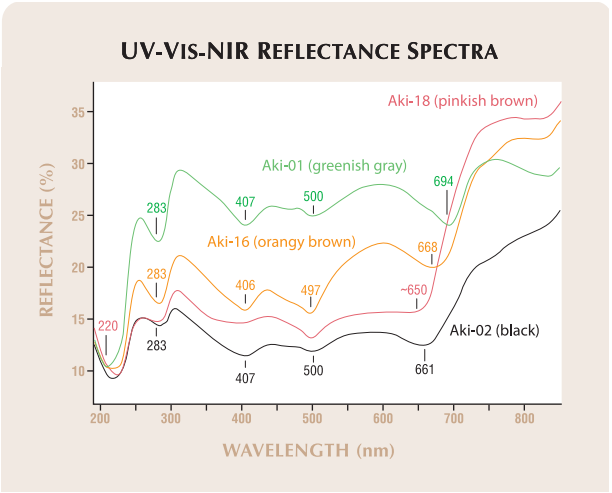

Figure 8. The UV-Vis-NIR reflectance spectra of the NCTCPs of various colors displayed a series of strong absorption bands, as well as a nearly flat baseline.

UV-Vis-NIR Reflectance Spectroscopy. Broad absorption bands centered at ~220, 283, ~407, 497–500, and ~650–694 nm occurred consistently in the NCTCPs (figure 8), though the height of the spectral baselines varied greatly. (In general, the darker a cultured pearl is, the lower its UV-Vis-NIR spectral baseline will be.) There was considerable variability among the NCTCP samples in both position and shape of the band at ~650–694 nm. The center of this band shifted as much as ~44 nm. In many of the brown NCTCPs, this band occurred as a shoulder (e.g., Aki-18 in figure 8), and was less distinct than bands recorded from gray NCTCPs. Notably, the baselines of the reflectance spectra were nearly horizontal for all the NCTCPs (both gray and brown), which means that the percentage of light reflectance at ~320 nm is very close to that at ~600 nm. (These two wavelength regions are relatively unaffected by absorption bands and, therefore, provide good reference points to judge the baseline.)

In the CCPs, the absorption bands described above were weaker in intensity or barely present. They also shifted slightly in position (figure 9). The band at 497–500 nm in the NCTCPs shifted consistently to higher wavelengths (510–529 nm) in the CCPs. The four "chocolate pearls" in figure 9 displayed similar brown colors, but the reflectance spectral baseline was inversely proportional to the tone of the brown color; that is, the baseline decreased as the tone increased. The baselines of all these spectra increased in general absorption toward lower wavelengths (higher energy); the reflectance percentage at ~320 nm was much lower than at ~600 nm. In the DTCPs, the spectral variations were even more dramatic. Only the peaks at ~220 and ~283–285 nm (and a weak absorption at ~700 nm in sample Bal-07) were clearly defined (figure 10). All other peaks observed in the NCTCPs and CCPs were generally less distinct (e.g., those located at 415 and 515 nm) or absent in the DTCPs. Instead, a broad absorption band ranging from ~320 to ~700

Figure 9. In contrast to the spectra shown in figure 8, the UV-Vis-NIR reflectance spectra of the CCPs exhibited baselines that increased in general absorption toward the low-wavelength (high-energy) side. The absorption bands (due to organic components) are less distinct, and some have shifted position, compared to those observed in the NCTCPs. Bal-57, Bal-60, and Bal-64 are orange-brown; Bal-70 is dark brown.

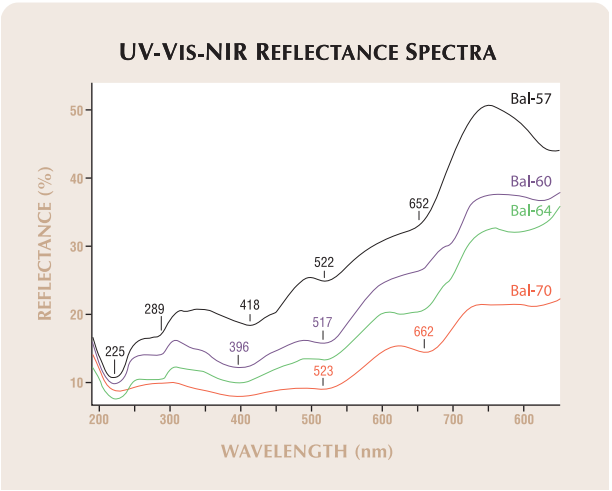

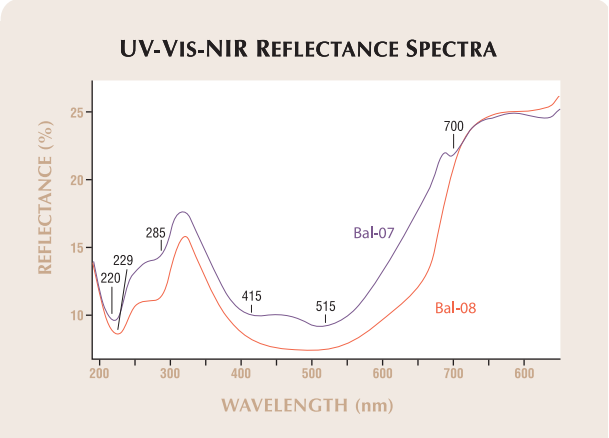

Figure 10. The UV-Vis-NIR reflectance spectra of these two DTCPs are very different from those of the NCTCPs and the CCPs. The spectra are dominated by a broad absorption band that ranges from ~320 to ~700 nm and is centered at ~500 nm.

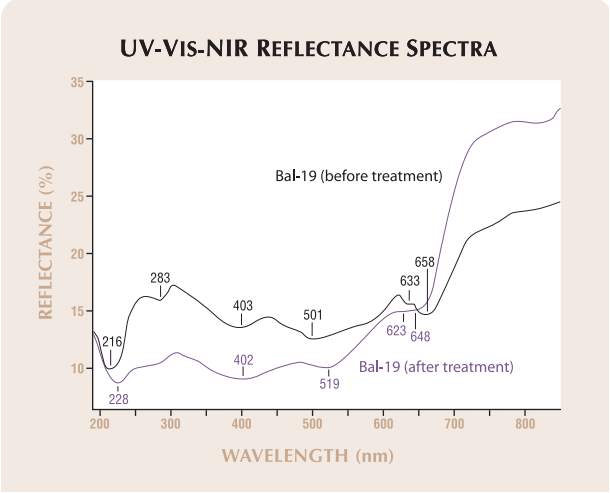

Figure 11. After treatment, the baseline of the UV-Vis-NIR reflectance spectrum of sample Bal-19 increased in general absorption toward the low-wavelength (high-energy) side; this appears to be a useful feature for identifying this type of "chocolate pearl." Also, absorption bands associated with organic components became less distinct.

nm and centered at ~500 nm was recorded. In contrast to the NCTCPs and CCPs, the reflectance percentage at ~320 nm in the DTCPs was much higher than at ~600 nm (again, see figure 10).

Clear variations in reflectance features before and after treatment were recorded in the four NCTCPs that were "chocolate" treated for this study (figure 11). The nearly flat baseline before treatment increased in general absorption toward the low-wavelength (high-energy) side of the spectrum, and the four absorption bands at 283, ~407, 497–500, and ~650–694 nm became broader and weaker and, consequently, less distinct. In addition, the band at ~407 nm shifted to 402–403 nm, the band at 497–500 nm moved 8–18 nm to higher wavelengths, and the band at ~650–694 nm shifted 10–14 nm to lower wavelengths. It should be pointed out that the ~407 nm band observed in figure 8 could occur as low as 403 nm in some NCTCPs (e.g., figure 11). After treatment, the reflectance percentage decreased dramatically in the region of 250–560 nm in three samples (Bal-02, Bal-18, and Bal-19), but this effect was less evident when the starting material was very dark in color (Bal-16).

Raman and Photoluminescence Spectroscopy. When excited by 488, 514, and 633 nm lasers, all the cultured pearls showed strong photoluminescence. Broad emission bands centered at ~620, 650, and 725–750 nm were observed (figure 12). Sharp Raman scattering peaks from carbonate components of the nacre overlaid these strong photoluminescence bands. Consistent luminescence features were observed in the spectra of the gray NCTCPs (12 samples), as well as in the spectra of those dominated by brown (seven samples). There were some subtle differences in the spectra of the gray and brown NCTCPs. Emission bands at 620 and 650

Figure 12. Strong photoluminescence was observed in both the NCTCPs and CCPs, with broad emission bands centered at ~620, 650, and 725–750 nm. The sharp peaks overlying those photoluminescence bands are caused by Raman scattering from carbonate components of the nacre. The spectra are shifted vertically for clarity.

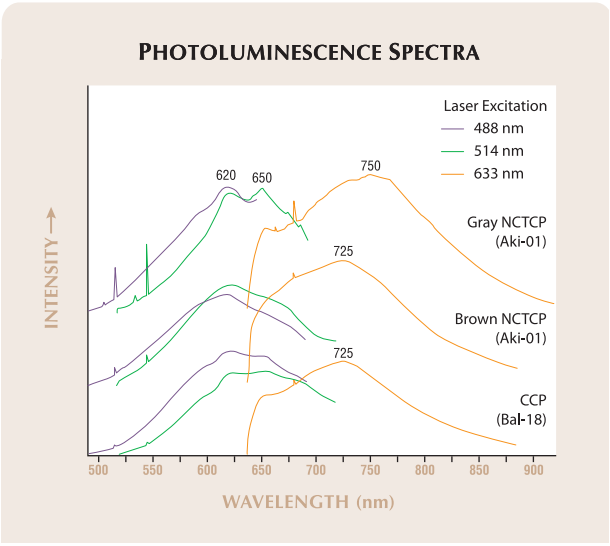

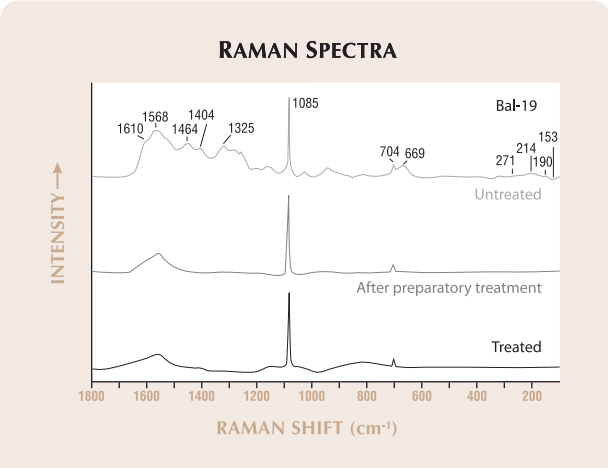

Figure 13. The Raman spectra of NCTCP Bal-19 changed considerably with the "chocolate" treatment, as the intensity of absorption due to organic components decreased significantly after the initial stage. These spectra were collected using 488 nm laser excitation and were normalized to the intensity of the Raman peak for aragonite at 1085 cm^{-1}. The spectra are shifted vertically for clarity.

nm in the brown NCTCPs were comparatively less distinct than in the gray NCTCPs. In addition, a band centered at ~750 nm in the gray NCTCPs occurred at ~725 nm in the brown NCTCPs. The brown NCTCPs showed photoluminescence features very similar to those of the 11 CCPs (again, see figure 12) and three DTCPs analyzed in this study (not shown in figure 12). When normalized to the intensity of the Raman scattering peak at 1085 cm^{-1} associated with the carbonate component of cultured pearls, the photoluminescence intensity of the CCPs was generally stronger than that of the NCTCPs. The weakest photoluminescence was observed in the DTCPs.

In the NCTCP samples, a strong peak at 1085 cm^{-1}, a moderate peak at 704 cm^{-1}, and weak peaks in the region of 300–100 cm^{-1} (271, 214, 190, 153, and 143 cm^{-1}) were observed in the Raman spectra of all samples when using 488 and 514 nm laser excitations (figure 13). Several broad bands were observed in the region of 1700–1300 cm^{-1}, with centers at approximately 1610, 1568, 1464, 1404, and 1325 cm^{-1}. A weak and broad peak also occurred at ~669 cm^{-1}. When 633 nm laser excitation was applied, the peak at 704 cm^{-1} resolved into a doublet at 701 and 705 cm^{-1}, and peaks in the region of 300–100 cm^{-1} became less distinct. The broad bands in the 1700–1300 cm^{-1} region and the peak at ~669 cm^{-1} also were present in the Raman spectra with 633 nm laser excitation.

In the four cultured pearls treated for this study, the intensity of the Raman peaks described above decreased significantly after the first stage of treatment: Most peaks were nearly absent below 1500 cm^{-1}, with the notable exceptions of the 1085 and 704 cm^{-1} peaks. Completion of the treatment depressed the peaks even further (again, see figure 13).

We also examined the full width at half maximum (FWHM) of the 1085 cm^{-1} peak in our samples from spectra collected using 514 nm laser excitation. In general, FWHM values were similar for all three sample categories: 5.4–7.8 cm^{-1} for the NCTCPs, 5.9–8.7 cm^{-1} for the CCPs, and 6.2–8.2 cm^{-1} for the DTCPs.

Chemical Analysis. In addition to the major element Ca, EDXRF analysis also detected a strong Sr signal in the nacre of all the cultured pearls tested. The only notable difference between the three groups of samples was that a strong Ag signal was recorded in the dyed cultured pearls. No other elements were observed with EDXRF.

Many trace elements were detected in the nacre of the cultured pearls with LA-ICP-MS, largely due to its much higher sensitivity (table 3). In the NCTCPs, relatively high concentrations of Na (5100–8200 ppm), Sr (1080–2320 ppm), K (66–410 ppm), Mg (66–274 ppm), and P (5.0–24.1 ppm) were detected. Traces of Li (0.33–0.58 ppm), B (12–24 ppm), Cr (1.5–4.5 ppm), Mn (up to 3.8 ppm), Zn (up to 18.7 ppm), Cd (up to 8.9 ppm), Ba (up to 2.9 ppm), Pb (up to 1.8 ppm), and Ag (0.01–1.8 ppm) were also detected. Other elements (again, see table 3) either were not detected or were near the detection limits for this instrument.

The composition of the CCPs was very similar to that of the NCTCPs. Concentrations of almost all elements fell in very similar ranges. One exception was the significantly lower concentration of K (average 47 ppm) in the CCPs compared to the NCTCPs (average 197 ppm). Another clear difference was the higher Pb concentrations in the CCPs (average 12.7 ppm) than in the NCTCPs (average 0.5 ppm). In before/after experiments, K concentrations in two samples (Bal-18 and Bal-19) decreased significantly after treatment. However, the opposite results were recorded in sample Aki-16. No significant variations in Pb were measured in the samples before and after treatment (table 3). In the DTCPs, elevated concentrations of Ag (1800–1870 ppm) and slightly enriched Sm (0.24–0.29 ppm; NCTCPs and CCPs had con-

TABLE 3. Representative composition of natural-color and "chocolate" treated Tahitian cultured pearls determined by LA-ICP-MS (ppm by weight).[a]

Sample no.	Li	B	Na	Mg	P	K	Cr	Mn	Zn	As	Sr	Ag	Cd	Ba	Pb
Natural-Color Tahitian Cultured Pearls (NCTCPs)															
Aki-04	0.42	18.55	6526	68.39	9.41	197.8	3.71	0.48	3.84	0.85	1181	0.12	0.05	0.71	0.52
Aki-05	0.44	18.57	6057	83.19	20.18	183.1	3.96	0.64	8.34	1.08	1240	0.02	0.15	2.80	0.45
Aki-06	0.36	13.79	5798	77.28	24.08	227.4	3.86	0.56	1.12	0.87	1081	0.01	0.04	0.30	0.17
Aki-07	0.37	16.93	6181	146.8	8.12	260.9	3.89	0.36	2.33	0.36	1203	0.04	8.92	0.38	1.24
Aki-08	0.35	15.61	5600	114.1	7.65	162.7	4.02	0.10	4.05	0.62	1778	0.06	0.14	0.44	0.36
Aki-14	0.35	13.83	5113	242.8	8.48	281.4	3.63	nd[b]	7.53	0.51	1845	0.13	1.02	0.81	0.24
Aki-15	0.45	15.83	5879	136.0	11.51	142.2	4.20	0.29	4.45	0.61	1891	0.16	0.03	0.82	0.35
Aki-16	0.34	15.88	5653	178.6	9.39	164.4	3.34	1.21	5.91	0.43	1932	0.16	0.21	0.62	0.34
Aki-17	0.35	16.31	6463	104.1	9.39	247.8	4.09	0.27	5.72	0.33	1581	0.20	0.09	0.52	0.41
Aki-18	0.46	13.02	7281	196.2	nd	314.9	2.64	0.44	5.83	0.53	1292	0.09	0.64	0.64	0.49
"Chocolate" Cultured Pearls (CCPs)															
Bal-24	0.35	13.78	5464	135.9	8.55	61.54	1.06	2.20	3.32	nd	1415	0.49	0.05	0.43	13.29
Bal-27	0.31	14.18	6487	115.9	13.13	44.30	4.45	6.93	3.64	0.02	1196	0.40	0.02	0.44	13.91
Bal-30	0.40	18.64	6762	82.51	10.51	58.85	4.88	1.19	5.47	nd	1473	0.19	nd	0.49	8.54
Bal-33	0.26	11.30	5487	175.5	8.51	15.14	3.61	1.00	1.77	nd	1095	0.06	0.03	0.50	11.03
Bal-36	0.26	11.01	5546	114.1	6.27	36.16	3.12	1.28	2.45	0.07	1283	0.15	0.02	0.22	8.20
Bal-37	0.31	13.18	6932	171.6	nd	21.88	5.17	1.31	6.01	0.35	1444	0.30	nd	0.60	16.02
Bal-40	0.34	8.75	5667	143.8	3.35	39.10	3.13	0.92	8.85	0.10	1514	0.20	0.00	0.92	22.25
Bal-43	0.36	14.30	5760	105.7	10.60	20.65	2.88	1.07	11.48	0.38	1106	0.27	0.00	0.38	19.62
Bal-46	0.44	14.19	6599	184.8	4.98	54.11	3.50	1.86	2.92	nd	1584	0.13	0.02	0.32	4.88
Bal-49	0.39	17.00	6177	119.8	15.85	55.89	3.39	2.66	15.99	0.00	1272	0.32	0.03	0.73	25.99
Dyed Tahitian Cultured Pearls (DTCPs)															
Bal-07	0.46	20.11	7720	104.2	10.34	85.79	3.60	0.72	4.22	0.32	1571	1800	0.22	2.66	0.17
Bal-08	0.51	19.11	7947	123.6	9.16	86.66	3.26	0.21	6.12	0.17	1188	1870	0.07	0.51	0.18
NCTCPs Before and After Treatment															
Bal-16	0.45	15.66	6387	142.5	5.60	74.45	3.23	2.67	16.56	nd	1970	0.11	0.13	1.09	0.26
Bal-16 (1st)	0.46	13.35	5724	179.0	nd	45.68	3.52	2.00	2.00	0.17	2223	0.12	0.02	0.68	0.37
Bal-16 (2nd)	0.73	11.93	6009	165.2	9.03	146.1	0.10	2.90	1.81	0.16	2458	0.04	0.06	0.76	0.31
Bal-18	0.37	13.88	6335	158.5	15.08	139.6	3.36	0.76	6.37	0.02	1723	0.03	0.08	3.14	0.45
Bal-18 (1st)	0.37	13.62	5867	164.9	nd	54.06	2.69	0.39	3.07	nd	1890	0.06	0.07	0.64	0.45
Bal-18 (2nd)	0.49	16.96	5874	195.4	19.84	59.45	0.07	0.93	1.47	0.06	1908	0.02	0.00	0.62	0.36
Bal-19	0.46	17.32	6694	139.2	8.50	118.6	3.70	1.20	4.79	0.03	1455	0.01	0.06	0.34	0.31
Bal-19 (1st)	0.38	15.88	5570	137.3	nd	30.11	3.49	1.39	1.53	0.06	1433	0.04	0.03	0.67	0.26
Bal-19 (2nd)	0.50	17.12	5739	158.1	17.03	92.36	0.03	1.92	0.70	0.10	1464	0.01	nd	0.18	0.19

[a] *Laser ablation parameters: 40 μm spot diameter, 30% (0.007 mJ) laser energy, 10 Hz repetition rate, and a 20 μm/s raster rate. NIST SRM 610 and 612 glass reference materials (Pearce et al., 1996) were used as external standards for calibration. The content of calcium throughout the nacre of all cultured pearls is nearly constant (~50 wt.% CaO), so this was employed as an internal standard in the data reduction for all samples. The following isotopes were monitored to determine elemental concentrations:* ^{7}*Li*, **^{9}Be**, ^{11}*B*, ^{23}*Na*, ^{24}*Mg*, ^{31}*P*, ^{39}*K*, ^{43}*Ca*, ^{44}*Ca*, **^{45}Sc**, **^{51}V**, ^{52}*Cr*, ^{55}*Mn*, **^{56}Fe**, **^{59}Co**, **^{60}Ni**, **^{65}Cu**, ^{66}*Zn*, **^{71}Ga**, **^{72}Ge**, ^{75}*As*, **^{82}Se**, **^{85}Rb**, ^{88}*Sr*, **^{89}Y**, **^{90}Zr**, **^{93}Nb**, **^{95}Mo**, ^{107}*Ag*, ^{111}*Cd*, **^{115}In**, **^{118}Sn**, **^{121}Sb**, **^{133}Cs**, ^{137}*Ba*, **^{139}La**, **^{140}Ce**, **^{141}Pr**, **^{146}Nd**, **^{147}Sm**, **^{153}Eu**, **^{157}Gd**, **^{159}Tb**, **^{163}Dy**, **^{165}Ho**, **^{166}Er**, **^{169}Tm**, **^{172}Yb**, **^{175}Lu**, **^{178}Hf**, **^{181}Ta**, **^{182}W**, **^{185}Re**, **^{197}Au**, **^{205}Tl**, ^{208}*Pb*, **^{209}Bi**, **^{232}Th**, *and* **^{238}U**. *Those isotopes marked in boldface roman type were not included in this table, as their concentrations were either below or near the instrumental detection limits.*

[b] *nd = not detected.*

centrations up to 0.05 ppm) were measured, while concentrations of other elements remained similar to those recorded for the untreated samples.

DISCUSSION

Pearl nacre consists of overlapping platelets of crystalline calcium carbonate ($CaCO_3$) in the form of aragonite, with the principal crystal axes of these platy crystals oriented at right angles to the surface. Various organic components occur between the aragonite platelets, producing a range of pearl colors (e.g., Kiefert et al., 2004; Strack, 2006).

Raman spectroscopy is a very effective technique for mineral identification, and in general Raman peaks are much sharper than overly strong photoluminescence bands. In aragonite, the most intense Raman peak occurs near 1085 cm^{-1}. Also in aragonite, a doublet may be observed at ~705 and ~701 cm^{-1}, whereas in calcite, the other common polymorph of $CaCO_3$, only a single band at ~711 cm^{-1} occurs (Urmos et al., 1991). Raman spectroscopic analysis of the untreated and treated Tahitian cultured pearls confirmed that aragonite is the only carbonate mineral component present in our samples (figure 13). As expected, no evidence for

calcite (i.e., 711 cm^{-1} peak) was observed in the Raman spectra of the natural-color, "chocolate" treated, or dyed Tahitian cultured pearls.

Other Raman features are attributed to various types of organic components, such as conchiolin and porphyrin (Goebel and Dirlam, 1989; Liu, 2003; Huang, 2006). The intensities of these organic component bands varied significantly among the NCTCPs, but they clearly increased with the tone of the cultured pearl colors (not shown in figure 13). After the first stage of treatment, the intensity of Raman peaks due to organic components decreased, especially below 1500 cm^{-1}; the peaks were even weaker after the treatment was completed (again, see figure 13).

For the most part, the Raman peak intensities of aragonite in the CCPs were comparable to those of the natural-color samples (figure 13). While many CCPs showed relatively weak organic peaks in the region of 1700–1300 cm^{-1}, a few samples like Bal-03 showed strong peaks (not shown). The weaker Raman scattering peaks for organic components in most of the CCPs, and the decreased intensity of these peaks in the four NCTCPs treated for this study, strongly indicate that the treatment mainly involves modifying the organic components between aragonite platelets (see figure 3).

In the DTCPs, we could not detect organic-related components and other Raman peak intensities were much weaker than in the NCTCPs and CCPs. Furthermore, the dyed cultured pearls did not show Raman peaks in the region 300–100 cm^{-1}, but they did have a broad band centered at ~141 cm^{-1}. A Raman band at 240 cm^{-1} previously reported in dyed cultured pearls by Kiefert et al. (2001) was observed in one sample (Bal-08), with 633 nm laser excitation only.

Infrared reflectance spectroscopy showed more complicated results. Most absorption features were consistent with aragonite, in particular the occurrence of the 1084 cm^{-1} peak, which is unique to aragonite. However, the 878 cm^{-1} band, which was consistently observed in all the untreated Tahitian cultured pearls, matched the peak position of calcite well. In aragonite, the same peak usually occurs at higher wavenumbers than 860 cm^{-1} (Weir and Lippincott, 1961; Adler and Kerr, 1962; Frech et al., 1980). We believe this peak is not related to calcite (as shown by the lack of calcite in the Raman spectra), so the cause of this relatively strong absorption at 878 cm^{-1} remains unclear. Our spectroscopic analysis revealed nearly identical Raman and infrared absorption features (figures 6, 7, and 13) for the aragonite peaks in both the untreated and "chocolate" Tahitian cultured pearls, indicating that the aragonite platelets in Tahitian cultured pearls remained basically unchanged during the "chocolate" treatment.

The vast majority of the NCTCPs showed weak yellow, orange, or greenish yellow fluorescence to long-wave UV. In contrast, the CCPs typically displayed characteristic reddish orange fluorescence. This difference in fluorescence was confirmed by the four cultured pearls processed for this study. The causes of the variation in fluorescence color are not clear; this may be attributed to modification of organic components or defects in the constitutional aragonite.

The dyeing of pearls with silver salts to turn them black has been practiced for many decades. First, the pearls are immersed in a silver nitrate solution ($AgNO_3$) for a period of time in a dark environment, and then they are exposed to a strong light source or are treated with hydrogen sulfate. The Ag-dyeing process leads to the deposition of AgO as extremely fine particles (Strack, 2006). These particles both strongly absorb visible light (inducing the dark brown coloration) and effectively block fluorescence, which is why no fluorescence could be detected in the DTCPs.

A relatively flat baseline in the UV-Vis-NIR reflectance spectra of the NCTCPs—with broad absorption bands at ~407, 497–500, and 650–694 nm—is consistent with the observed gray or brown colorations (again, see figure 8). The absorption band at ~283 nm is derived from protein contained in conchiolin, a common feature of all cultured pearls (see, e.g., Iwahashi and Akamatsu, 1994). The absorption bands at ~407 and 497–500 nm are derived from porphyrin pigment. The ~407 nm absorption is called the "Solet band," which is common to all porphyrins (see, e.g., Iwahashi and Akamatsu, 1994). Depending on the fine structure of the porphyrin, this band can occur anywhere from 390 to 425 nm (Britton, 1983). The ~650–694 nm absorption band is derived from black pigment in cultured pearls. In addition, there are spectroscopic variations among geographic sources of "black" cultured pearls. For example, the 661–694 nm band, which we observed consistently in our Tahitian cultured pearls, was not reported in Mexican cultured pearls (Kiefert et al., 2004), even though they showed very similar coloration. The presence of these bands provides a good indication for substantial quantities of organic components.

Our analysis of a large number of CCPs revealed that the baseline of their UV-Vis-NIR reflectance spectra consistently increased in general absorption toward lower wavelengths (higher energies; figure 9). This absorption increased over the whole region of visible light, resulting in the intense brown coloration. A decrease in intensity (or virtual absence) of these three absorption bands in the 300–700 nm region after treatment, as observed in the CCPs and the four cultured pearls treated for this study (figures 9 and 11), also indicates that the organic components are dramatically modified. Observation of such modified spectra provide good evidence for bleaching during the treatment.

Pearl formation is mainly a process of deposition of aragonite by mollusks. Tahitian cultured pearls, like all of the samples in this study, form in seawater, which contains minor or trace amounts of various elements. Since the geochemical properties of strontium are very similar to those of calcium, it is common for pearls to contain relatively high amounts of Sr (see table 3). Seawater also contains significant amounts of sodium and potassium; their presence in the cultured pearls was well reflected in the compositions we measured with LA-ICP-MS. However, little information is available regarding the incorporation of Na and K in pearls. While Na and K may partially enter the aragonite lattice, these elements also may be enriched at the interfaces between aragonite platelets. It is interesting to note that the untreated NCTCPs also contained traces of Ag (up to 1.8 ppm by LA-ICP-MS analysis, but not detectable by EDXRF). However, much higher concentrations of Ag are needed to induce any observable coloration, as in the Ag-dyed cultured pearls.

LA-ICP-MS analysis of NCTCPs and CCPs (table 3) revealed that both groups had very similar compositions, except for less potassium and relatively higher concentrations of lead in the CCPs. A decrease in K concentration was correlated with some samples treated in this study (table 3), but contradictory results were also observed. In addition, the samples analyzed before and after treatment did not show any detectable variation in Pb concentrations. When not locked into a crystal lattice, K can be a very mobile element (Albarede and Hofmann, 2003). The lower abundance of K in the CCPs strongly indicated that most of the K in the NCTCPs is located at the interfaces between aragonite platelets and can be partially removed in the treatment. Nevertheless, the differences in K and Pb concentrations between NCTCPs and CCPs were not confirmed in the before/after treatments. The causes for these inconsistencies are not clear. On the basis of these data and observations, it is reasonable to believe that color changes caused by the "chocolate" treatment are mainly related to the reorganization of organic pigments that are present between the aragonite platelets, without the introduction of a foreign coloring agent. The chemical data suggest that the treatment did not add any chemical elements and, therefore, is fundamentally different from the Ag-dyeing treatment.

IDENTIFICATION

Identification of Ballerina-treated "chocolate" cultured pearls requires a combination of gemological observation, spectroscopic analysis, and trace-element composition. Natural-color cultured pearls rarely show intense brown coloration without a distinct orient or rosé overtone (Scarratt, 1984). Suspicion should be raised for samples that show pronounced "chocolate" coloration.

Most (157 of 160 samples) of the Ballerina CCPs we studied showed a weak-to-moderate reddish orange fluorescence to long-wave UV radiation. The remaining three samples showed greenish yellow fluorescence to long-wave UV, which is similar to the reaction of many untreated Tahitian cultured pearls. Consequently, reddish orange fluorescence to long-wave UV is a useful indication of treatment, but caution must be exercised since there are exceptions. While DTCPs and CCPs can have a similar color appearance, DTCPs are usually inert to both long- and short-wave UV radiation.

Spectroscopic and chemical analyses supply information that is essential for identification. The high concentrations of Ag in dyed cultured pearls can be detected easily with either EDXRF or LA-ICP-MS. Relatively low concentrations of K and elevated contents of Pb, combined with a concentration of Ag consistent with NCTCPs (i.e., <2 ppm) may provide indications of this type of "chocolate" treatment. UV-Vis-NIR reflectance spectroscopy is also very useful due to the systematic differences between NCTCPs, CCPs, and DTCPs. An important feature of the reflectance spectra of brown NCTCPs is that the baseline is nearly flat, similar to that seen with gray NCTCPs. However, the baselines of all the CCPs we examined always increased in general absorption toward the low-wavelength (high-energy) side of the spectra. Untreated cultured pearls from Mexico and South America may show a

similar reaction to long-wave UV as CCPs (Kiefert et al., 2004); however, we may expect quite different reflectance spectra in the UV-Vis-NIR range. In addition, very weak or no absorptions at ~407, 497–500, and 650–694 nm provide good evidence of bleaching treatment. Strong photoluminescence with peaks at ~620 nm and ~725 nm relative to Raman peaks from aragonite is a good indication of bleaching treatment, but it is not conclusive.

CONCLUSION

In addition to the well-known Ag-dyeing method, brown "chocolate"-colored cultured pearls can be produced using a newly developed bleaching treatment. This method is able to turn black cultured pearls from Tahiti (and very likely other sources) with less attractive or non-uniform colors into those with uniform and pleasing brown colors, and potentially increase their market value. No chemical evidence of foreign coloring agents was detected following Ballerina's bleaching process. Treated brown cultured pearls, either bleached or dyed, can be identified based on a combination of their gemological properties, chemical composition, and spectroscopic features.

It is important to note that treated cultured pearls with similar "chocolate" colors are also present in the market from sources other than Ballerina Pearl Co. (figure 14). Since the treatment process is proprietary, and the starting materials may come from various sources, there is no guarantee that "chocolate pearls" from other companies will show analogous results.

Figure 14. The "chocolate pearls" now in the marketplace are being produced by a number of different companies. These attractive cultured pearls range from 11.0 to 15.7 mm. Courtesy of Emiko Pearls International; photo by Robert Weldon.

ABOUT THE AUTHORS
Dr. Wang (wuyi.wang@gia.edu) is a research scientist, Ms. Hyatt is a staff gemologist, and Mr. Hall is manager of analytical research services, at the GIA Laboratory, New York. Mr. Scarratt is director of GIA Research (Thailand) in Bangkok. Dr. Shen is a research scientist at the GIA Laboratory, Carlsbad.

ACKNOWLEDGMENTS
The authors are grateful to Abe Auerbach of the Ballerina Pearl Co. in New York, as well as Emiko Pearls International in Seattle, for supplying treated cultured pearl samples for examination. Special thanks to Tom Moses of the GIA Laboratory (New York) for many fruitful discussions and Dr. Christopher Breeding of the GIA Laboratory (Carlsbad) for help in this study. The authors are also grateful to Shigeru Akamatsu of Mikimoto & Co. (Tokyo), Dr. Henry Hänni of the SSEF Swiss Gemmological Laboratory (Basel), and Dr. Lore Kiefert of the AGTA Gemological Testing Center (New York) for their constructive comments and suggestions, which helped improve this article significantly.

REFERENCES

Adler H.H., Kerr P.F. (1962) Infrared study of aragonite and calcite. *American Mineralogist*, Vol. 47, pp. 700–717.

Albarede F., Hofmann A.W. (2003) *Geochemistry: An Introduction*. Cambridge University Press, Cambridge.

Better techniques improve brown pearls (2006) *Jewellery News Asia*, No. 262, p. 60.

Britton G. (1983) *The Biochemistry of Natural Pigments*. Cambridge University Press, Cambridge.

Frech R., Wang E.C., Bates J.B. (1980) The IR and Raman spectra of $CaCO_3$ (aragonite). *Spectrochimica Acta*, Vol. 36A, pp. 915–919.

Gemological Institute of America (2000) GIA Pearl Grading Color Reference Charts. Carlsbad, CA.

GIA identifies three types of brown pearls (2006) *Jewellery News Asia*, No. 265, p. 80.

Goebel M., Dirlam D.M. (1989) Polynesian black pearls. *Gems & Gemology*, Vol. 25, No. 3, pp.130–148.

Huang Y.L. (2006) Visible absorption spectrum representation of Tahitian black pearls and treated pearls. *Journal of Gems and Gemmology*, Vol. 8, No. 1, pp. 5–8.

Iwahashi Y., Akamatsu S. (1994) Porphyrin pigment in black-lip pearls and its application to pearl identification. *Fisheries Science*, Vol. 60, No. 1, pp. 69–71.

Kiefert L., Hänni H.A., Ostertag T. (2001) Raman spectroscopic applications to gemmology. In I.R. Lewis and H.G.M. Edwards, Eds., *Handbook of Raman Spectroscopy*, Marcel Dekker, New York, pp. 469–489.

Kiefert L., Moreno D.M., Arizmendi E., Hänni H.A., Elen S. (2004) Cultured pearls from the Gulf of California, Mexico. *Gems & Gemology*, Vol. 40, No. 1, pp. 26–39.

Liu W.D. (2003) Characteristics of Tahitian black pearls and their application in identification. *Journal of Gems and Gemmology*, Vol. 5, No. 1, pp. 1–4.

Pearce N.J.G., Perkins W.T., Westgate J.A., Gorton M.P., Jackson S.E., Neal C.R., Chenery S.P. (1996) Application of new and published major and trace elements data for NIST SRM 610 and NIST SRM 612 glass reference materials. *Geostandards Newsletter*, Vol. 20, No. 2, pp. 115–144.

Sanchez L. (2004) Trade raises questions about chocolate pearls. *Jewellery News Asia*, No. 241, pp. 160, 162.

Strack E. (2006) *Pearls*. Ruhle-Diebener-Verlag, Baden-Baden, Germany.

Study shows chocolate pearls are "stained" (2006) *Jewellery News Asia*, No. 265, p. 78.

Urmos J., Sharma S.K., Mackenzie F.T. (1991) Characterization of some biogenic carbonates with Raman spectroscopy. *American Mineralogist*, Vol. 76, No. 3–4, pp. 641–646.

U.S. gem labs seek to uncover the process behind brown pearls (2004) *Jewellery News Asia*, No. 241, p. 162.

Weir C.E., Lippincott E.R. (1961) Infrared studies of aragonite, calcite, and vaterite type structure in the borates, carbonates, and nitrates. *Journal of Research of the National Bureau of Standards A. Physics and Chemistry*, Vol. 65, pp. 173–183.

Zachovay M. (2005) Gem News International: "Chocolate" Tahitian cultured pearls. *Gems & Gemology*, Vol. 41, No. 2, pp. 183–184.

Thank You Reviewers

GEMS & GEMOLOGY requires that all articles undergo a peer review process in which each manuscript is evaluated by at least three experts in the field. This process is vital to the accuracy and readability of the published article, but it is also time consuming for the reviewer. Because members of our Editorial Review Board cannot have expertise in every area, we sometimes call on other experts to share their intellect and insight. In addition to the members of our Editorial Review Board, we extend a heartfelt thanks to the following individuals who reviewed manuscripts for *G&G* in 2006.

Mr. Charles Carmona
Dr. Richard Grigg
Mr. Matthew Hall
Mr. Hertz Hasenfeld
Dr. Frank Hawthorne
Mr. John King
Ms. Elise Misiorowski
Dr. Andrew Rankin
Dr. Ilene Reinitz
Dr. Karl Schmetzer
Dr. Dietmar Schwarz
Mr. George Solario
Dr. Jennifer Stone-Sundberg
Dr. Wuyi Wang